Original Article

Effect of laser energy density on porosity and microstructural features of Inconel 625 alloy produced by selective laser melting

Rıdvan YAMANOĞLU[1] , **Egemen AVCU**[2] , **Hasan İsmail YAVUZ**[*1] , **Mertcan KIRAÇ**[3] ,
Ümit Gencay BAŞÇI[1] , **Enes Furkan SEVİNÇ**[3] , **Ertuğrul BAYRAM**[1]

[1]Department of Metallurgical and Materials Engineering, Kocaeli University, Kocaeli, Türkiye
[2]Ford Otosan Ihsaniye Automotive Vocational School, Kocaeli University, Kocaeli, Türkiye
[3]R&D Department, Ermaksan, Bursa, Türkiye

ABSTRACT

Additive manufacturing (AM) is a state-of-the-art technique that enables the production of advanced materials with complex designs. Nonetheless, many challenges remain in the additive manufacturing of nickel-based superalloy components, especially in revealing the effects of processing parameters on their microstructural characteristics. The present study aims to reveal the effect of laser energy density (LED) on porosity and microstructural features of the Inconel 625 (IN625) alloy produced by SLM using a newly developed SLM metal additive manufacturing machine (ENAVISION 250, Ermaksan, Türkiye) for the first time. The layer thickness was selected as 30 µm for all samples. The samples were produced with 9 different LED values (ranging between 0.78 and 2.80 J/mm) using a 350 W laser power and scanning speeds ranging from 125 to 450 mm.s^{-1}. Optical microscope images of the polished and etched samples in the XY, XZ, and XY planes were studied. The influence of the LED intensity on both the quantity and morphology of the pores in the structure was evaluated. Spherical-shaped pores were identified in samples with LED levels of 1 J/mm and above. The porosities within the structure increased after the LED value attained 1.17 J/mm, simultaneously revealing an increase in pore size with the increasing LED value. The application of high energy density to the powders led to an increase in the solubility of gas, resulting in the formation of numerous spherical pores. This study indicated that the optimum LED value for IN625 alloy with a layer thickness of 30 µm is 0.78 J/mm. The study offers significant insights into the correlation between LED value and the microstructural characteristics of superalloys fabricated by SLM, thereby aiding in the optimisation of SLM processing parameters for diverse components across various sectors, including aerospace, aviation, automotive, and defence industries.

Cite this article as: Yamanoğlu, R., Avcu, E., Yavuz, H. İ., Kıraç, M., Başçı, Ü. G., Sevinç, E. F., & Bayram, E. (2024). Effect of laser energy density on porosity and microstructural features of Inconel 625 alloy produced by selective laser melting. *J Adv Manuf Eng*, 5(2), 00–00.

INTRODUCTION

Today, additive manufacturing (AM) is a popular technology that produces unique and complex components for various applications. AM offers many advantages, such as cost-effective products, strong and lightweight parts, flexible designs, minimal material waste, ease of access, and rapid design and production [1]. This has resulted in an extraordinary expansion of AM technology's application area in just thirty years, making it an innovative alterna-

*Corresponding author.
*E-mail address: hasanismail.yavuz@kocaeli.edu.tr

tive in production and logistics processes. Investments in AM technology have increased the market volume from 4 billion dollars in 2014 to over 21 billion dollars in 2020. Researchers predict that the growth rate in AM technology will increase year by year and reach 110 billion dollars in 2033 [2]. Many developments in AM technologies and materials have stimulated the market for further investment in various sectors, such as biomedical, aerospace, space, and automotive, which have played an important role in increasing market volume [3]. 3D machine manufacturers and raw-material-producing companies play an essential role in the development of the AM sector. Analysis of the machine manufacturers in the AM market reveals that the leading producers are Sweden, Germany, France, the United Kingdom, Japan, the United States, and Canada [4], demonstrating that many developed countries have already invested in AM technologies.

The production of alloys with complex microstructural features, such as IN625, is challenging due to the processing conditions of additive manufacturing, e.g., rapid solidification and layer-by-layer processing [5, 6]. Producing high-density components is critical since the mechanical properties of produced parts are highly related to the density of processed components. Enhanced porosity elevates the stress per unit volume within the material and reduces its mechanical characteristics [7]. To achieve the target density, it is essential to optimise the characteristics of the raw materials, including particle shape, surface morphology, particle size distribution, and internal porosity. This optimisation is crucial in producing metallic components using laser powder-bed fusion (LBPF) methods [8–11]. For instance, Field et al. [12] obtained tungsten powder with two different characteristics by chemical methods and plasma atomization. Both tungsten powders possess high purity; however, they exhibit variations in size distribution, morphology, thermal characteristics, and flow properties. The study found that the material displayed a higher density when utilising powders produced through plasma atomisation, as these powders demonstrated superior sphericity and a more uniform particle size distribution than those produced via the chemical method.

Selective laser melting, the most industrially popular method among LPBF technologies, is a AM method that produces 3D components by melting a bed of fine metallic powders layer by layer using a laser beam [4, 13, 14]. It is a highly complex technology controlled by multiple process parameters such as layer thickness, laser power, scanning strategy and speed, chamber atmosphere, support structures, and building orientation [15]. Four basic parameters, such as laser power P [W], scanning speed v [mm.s], distance between two consecutive laser scans h [mm], and layer thickness d [mm], are utilised to calculate the "Laser Energy Density" (LED=P/v.h.d) [J/mm] [16, 17]. These parameters significantly determine material performance because they alter the heat input to the powders per unit weight. By increasing the scanning speed or reducing the laser power, the linear energy density of the laser input decreases [18–20].

The LED value affects the densification process and is critical in determining the density-to-porosity ratio and the material's final microstructure [21, 22]. For example, Sadowski et al. [23] produced Inconel 718 at a constant scanning speed of 200 mm/s and different laser powers between 40 W and 300 W. The cross-sectional images of the laser scanning lines showed that the laser power of 40 W was insufficient for melting due to the insufficient energy, leading to void in the microstructure. Upon increasing the laser power to 100 W, it was noted that complete wetting did not occur, and pilling continued. Upon increasing the laser power to 150 W, pilling was eliminated, and it was established that the laser strength could melt three layers of powder. With an increase of laser power to 200 W and 300 W, the stability of the melt pool diminished, resulting in a reduced solidification rate. Similarly, Yi et al. [24] investigated the effect of LED value (values ranging from 0.1 J/mm to 0.3 J/mm) on the microstructural properties of IN718 alloy produced by SLM. It was determined that the number and size of pores were minimised at the 0.2 J/mm LED value. When the line laser energy increased to 0.3 J/mm, pores were detected in the inter-pool regions due to poor overlap of the melt pool boundary, resulting in a decrease in mechanical properties.

Based upon the presented literature review, it is necessary to determine the LED value range to produce demanding engineering components with superior mechanical properties and optimised microstructural features. The present study aims to reveal the effect of laser energy density on porosity and microstructural features of the Inconel 625 alloy produced by SLM using a newly developed SLM metal additive manufacturing machine (ENAVISION 250, Ermaksan, Türkiye), for the first time. Thus, a wide range of LED values are selected to understand the influences of LED values on the porosity and microstructural features of the IN625 alloy. It is aimed to establish a clear correlation between the LED value and the porosity ratio and the optimum LED value for a layer thickness of 30 μm for producing IN625 alloy, which has yet to be studied in the literature. Thus, the study also provides significant outcomes for the academic and commercial use of the Ermaksan Enavision 250 AM Machine, contributing to the field of metal additive manufacturing in Türkiye.

MATERIALS AND METHODS

Materials

Ermaksan A.Ş. supplied gas-atomised IN625 powder, and the chemical composition, particle size, and particle shape of the metal powder were analysed. The chemical composition was measured using an Agilent ICP-OES instrument. Table 1 shows the chemical composition of the IN625 alloy powder used in the study according to the ASTM F3056 standard. The particle size distribution (PSD) of IN625 powder was measured using a Malvern Mastersizer 3000E. According to the analysis, the average

Table 1. Chemical composition of IN625 alloy powder

Elements	Ni	Cr	Mo	Nb	Mn	Fe	Si	Al	C
ASTM F3056 (wt. %)	Rest	20–23	8–10	3.1–4	max. 0.50	max. 5	max. 0.50	max. 0.4	max. 0.10
This study (wt. %)	Rest	21.5	8.9	3.5	0.02	1.07	0.07	0.15	0.04

Table 2. LED values for the AM production of IN625 alloy

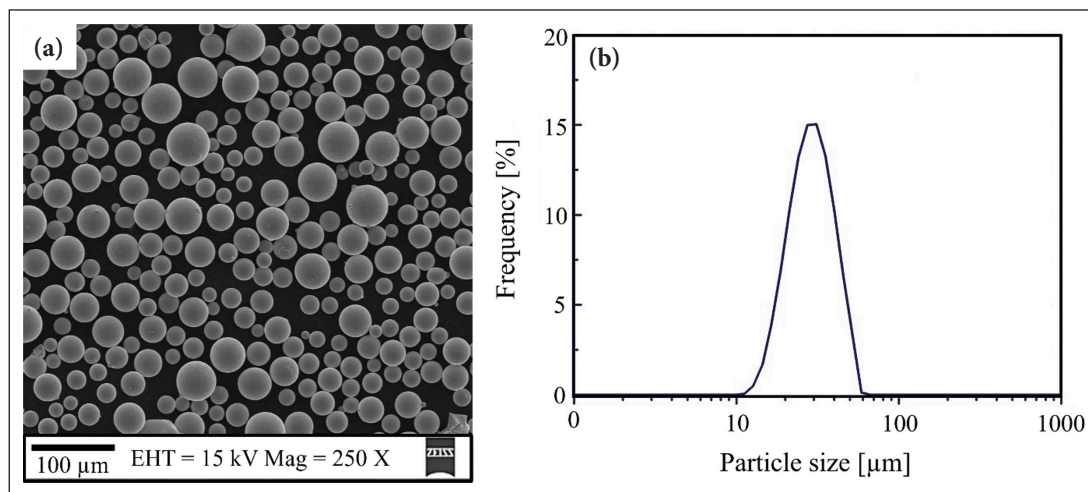| Sample code	1	2	3	4	5	6	7	8	9
Laser power (W)	350	350	350	350	350	350	350	350	350
Laser scanning rate (mm/s)	450	400	350	300	250	200	175	150	125
LED value (J/mm)	0.78	0.88	1.00	1.17	1.40	1.75	2.00	2.33	2.80

LED: Laser energy density

Figure 1. SEM images and particle size distribution of IN625 powders; **(a)** particle morphology **(b)** particle size distribution.

particle size (D50) was 30.7 μm. IN625 powder images were examined using a ZEISS brand GEMINI SEM 300 model electron microscope. Particle size distribution and powder images are given in Figure 1.

Additive Manufacturing of Samples

Considering the challenges associated with SLM processing, we have performed initial investigations, including single-line scanning studies under various conditions, to achieve sufficient melting, wettability, and a linear metal line concerning layer thickness. Thus, all parameters were selected based on insights derived from preliminary studies and a review of the relevant literature. In this work, density optimisation was performed, which is among the first and most critical factors regarding material performance in SLM production. Density values varying according to the LED value were measured, and the maximum density was tried to be obtained. LED value is expressed as the ratio of laser power to scanning speed. With the laser power measured in watts (joule/s) and scanning speed in mm/s, the linear energy density (LED) value is calculated in joule/mm. This value represents the energy applied by the laser to the powder per millimetre. This energy influences metallurgical phenomena such as melt pool size, width, solidification rate, atomic diffusion, and grain size [25, 26]. The most important parameter we use in IN625 part production is the LED value that maximises the intensity. The single-line scanning study was conducted to determine the ideal LED (j/mm) value for achieving sufficient melting, wettability, and a linear metal line in relation to the layer thickness. The LED values determined for production in the study are shown in Table 2. The production process with SLM was carried out with an Ermaksan ENAVISION 250 SLM machine. The device is equipped with a standard IPC laser, featuring a laser beam diameter of 0.4 mm. The scanning range is 0.1 mm with a rotation of 67 degrees. The machine possesses a production area volume of 250 mm x 250 mm x 250 mm with an adjustable layer thickness precision of 1 μm. The production was carried out under an argon atmosphere.

Microstructural Characterisation

The XY, YZ, and XZ planes of the samples produced for 9 different LED values were analysed. This study investigated the effects of SLM production parameters on the melting pool and grain shape of each sample produced with varying values of LED. Various metallographic processes were applied to the samples before microstructural analysis. Firstly, samples with dimensions of 10x10x30 mm³ were cut in XY, XZ, and YZ planes with a METKON brand microcut 150 model precision cutting device. The specimens were then
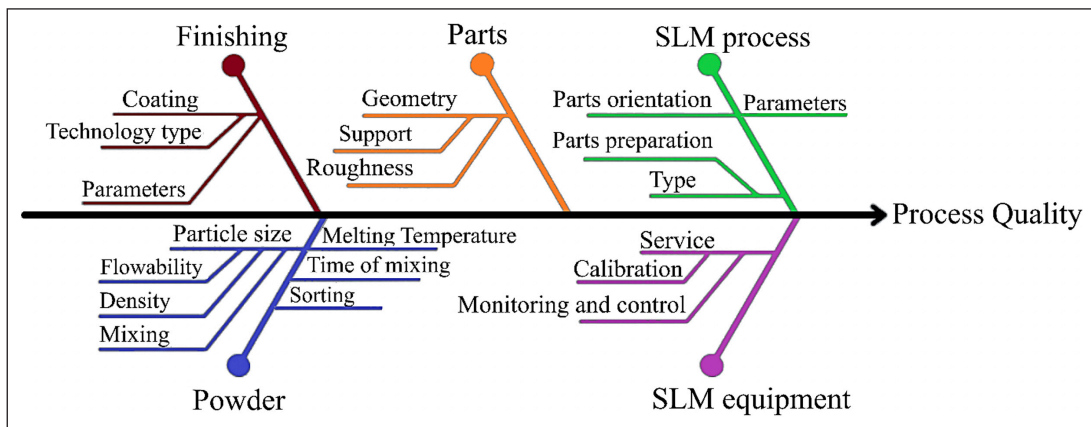
Figure 2. Schematic diagram of SLM process quality. Reproduced under the terms of the CC-BY Creative Commons Attribution 4.0 International License [36]. Copyright 2018, The Authors, published by IOP Publishing.

baked in a cold mold. The samples were grinded with 320, 600, 1000, and 2000 grit SiC abrasives (Akasel, Denmark). Then, a gradual polishing was performed with 9, 3, and 1 mm diamond solutions (Akasel, Denmark). The samples were etched with 15 ml HCl + 10 ml HNO_3 + 5 ml CH_3COOH solution for 180 s at room temperature to reveal the microstructure. Microstructural images in polished and etched positions were analysed in three dimensions with an Olympus BX41M-LED model optical microscope. Finally, the final densities of the samples were determined by measuring them with an AND GR-200 brand precision balance according to the Archimedes method [27].

RESULTS AND DISCUSSIONS

The recent literature indicates that the mechanical properties of materials in laser powder bed metal additive manufacturing technologies are influenced by various process parameters, including particle properties, machine properties, production parameters, part variables, and post-production process parameters [28–32]. Figure 2 depicts a schematic illustration of the factors that influence the quality of parts in the SLM method. Powder raw material affects part quality depending on its properties, such as chemical composition, particle size, particle morphology, particle size distribution, fluidity, and packaging factor [33]. It is desirable that the powder raw material's chemical composition be low in terms of oxygen and hydrogen content [34]. On the other hand, it is preferred that the powder particles be in the range of 15-60 μm to have a high fluidity and packaging factor for the powders laid layer by layer. Another powder-induced parameter that affects part quality is particle shape. Particle morphology affects metal powder fluidity, packing factor, and spread powder layer roughness. In order to ensure high fluidity, the particles used in this method are required to have a spherical shape [35]. In addition, a high packing density offers more homogeneous melting at lower laser energy.

The powder's particle size distribution is another raw material-based parameter that affects packing density. It is expected that the particles should be distributed over a
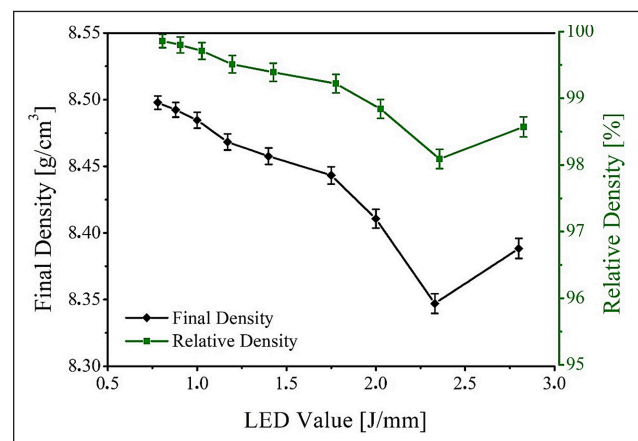

Figure 3. Final and relative densities of samples produced at different LED values. The relative densities of the samples are determined by dividing the final densities of the samples by the theoretical density.

wide size range instead of a single size. The final and relative density values of the samples produced in the study are given in Figure 3. As can be seen, the highest final density value was measured in the sample produced with a 0.78 J/mm LED value. As the LED value increased, the final densities decreased. When the relative density values were analysed, it was determined that the sample produced with a 0.78 J/mm LED value reached 99.86%. This ratio is well above the average density value seen in the samples produced with SLM. Microstructural characterisation processes were carried out in the study to verify the measured density values. Polished and etched specimen images in all axes (XY, XZ, and YZ) are given in Figure 4 and Figure 5, respectively. Laser power, scanning speed, distance, pattern, powder bed temperature, and atmospheric oxygen content affect SLM part quality [37]. According to the layer thickness selected during manufacturing, the metal powder emitted by the recoater interacts with the laser while moving by the machine software according to the cross-section of the component. During this interaction, a very small melting pool is formed, and the melting pool solidifies very quickly. The solidification speed is approximately 10^4-10^6 °K/s [38].
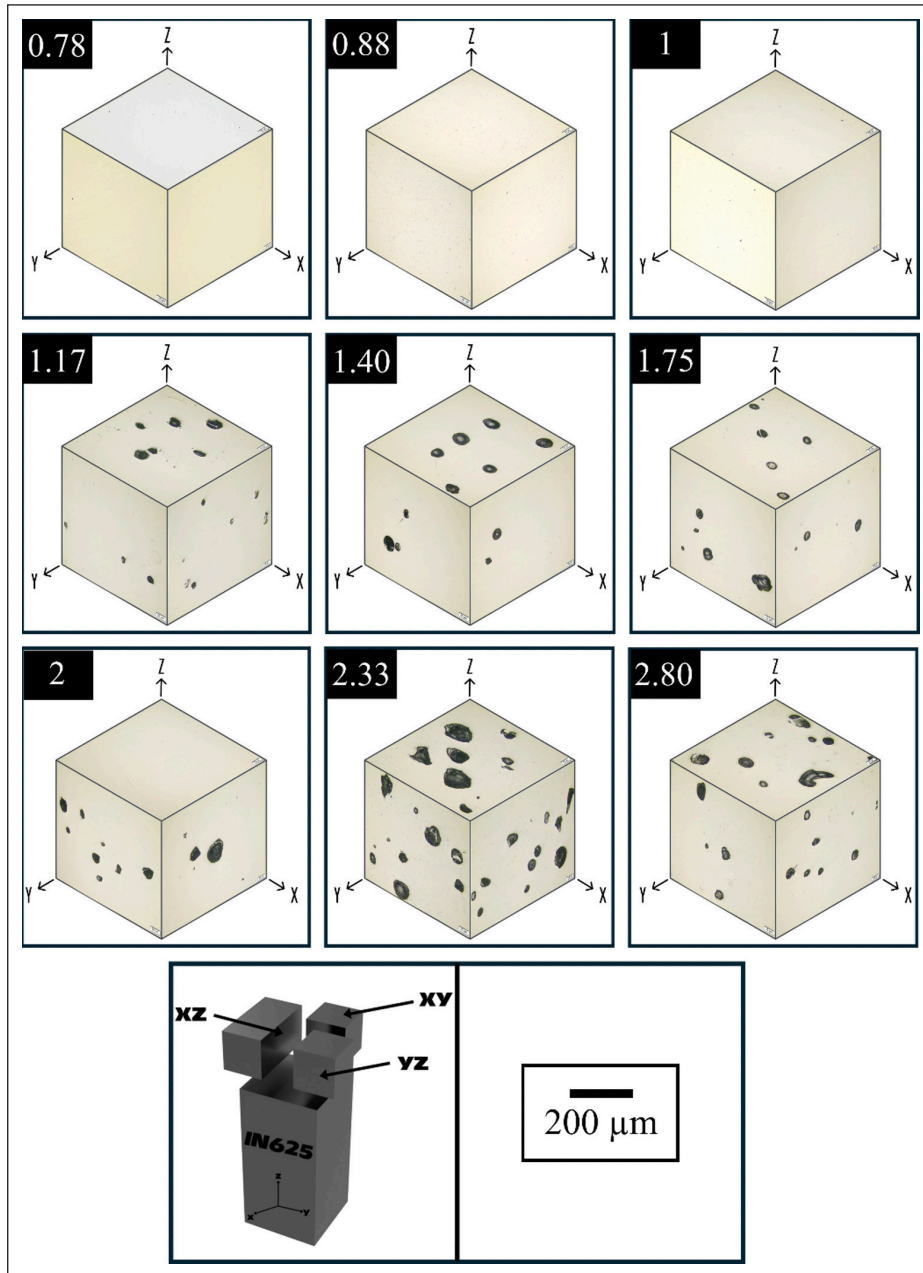
Figure 4. 3D display of three-axis polished microstructure images according to LED values: The numbers in the upper left corner represent the LED values.

The melt pool formed by laser-powder interaction and cooling and metallurgical events during solidification affect part quality and mechanical properties. Density measurement and microstructural analysis of the produced material are the first study outputs to optimize parameters. Microstructural analysis can determine the types of porosities formed by laser-powder interaction in SLM materials, while material density gives us an idea of the number. Information about the pore morphology will help determine the suitability of the applied LED values. Low LED values cause a lack of fusion, leading to many porosities in the internal structure [39]. However, negligible pore formation is observed at medium and high LED values. Regarding mechanical properties, the pore structure formed at low LED values is considered more dangerous than the structure obtained at medium and high LED values [40]. The material's fatigue strength is considerably reduced by the pore morphology, particularly at low LED values, as indicated by the relevant research [41]. Therefore, some critical parameters should be optimized to produce metallic materials with superior performance by SLM. Figure 4 gives the 3D display of three-axis polished microstructure images. When Figure 4 is analysed, many macro-sized porosities are observed in the samples produced at 1 J/mm LED value for IN625. The increase in gas solubility in the structure due to high energy density increased the amount of porosity [42, 43].

The solubility of gas in the liquid metal increases as a result of the elevated temperature. As a result of the exceptionally rapid cooling rate, the gas dissolved in the solidified
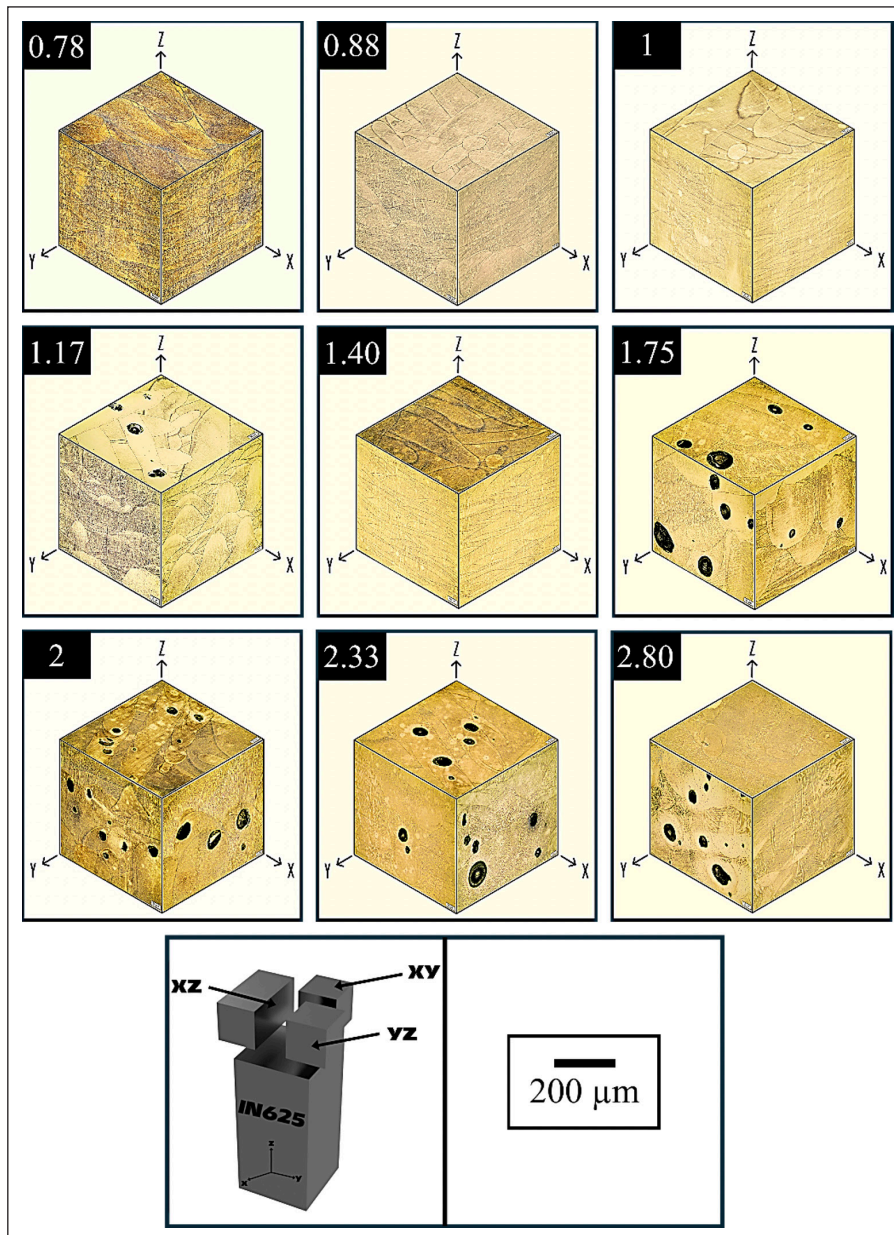
Figure 5. 3D display of three-axis etched microstructure images according to LED values: The numbers in the upper left corner represent the LED values.

metal becomes trapped and creates spherical pores. These porosities are known as gas bubbles [44, 45]. Due to the melting temperature of the IN625 alloy (1350 °C), porosities were formed in the structure at 1.17 J/mm and higher LED values in the study. Figure 5 gives the 3D display of three-axis etched microstructure images. Figures 4 and 5 demonstrate that porosities are not confined to a single plane but occur in all XY, XZ, and YZ planes. Consequently, the microstructures analysed in the study are found to be consistent with the measured density values (Fig. 3).

Materials produced with SLM can exhibit three distinct types of cracks. These cracks can be categorized as solidification cracking occurring along the solidifying layer due to tensile stress caused by thermal contraction, liquefaction cracking affecting the partially molten zone, and delamination [40]. Another problem encountered in
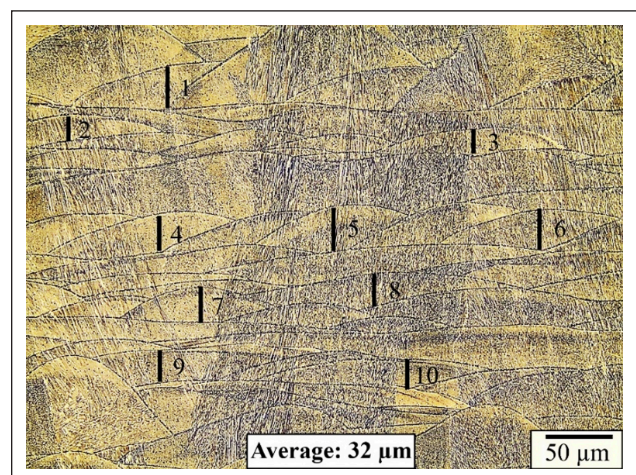

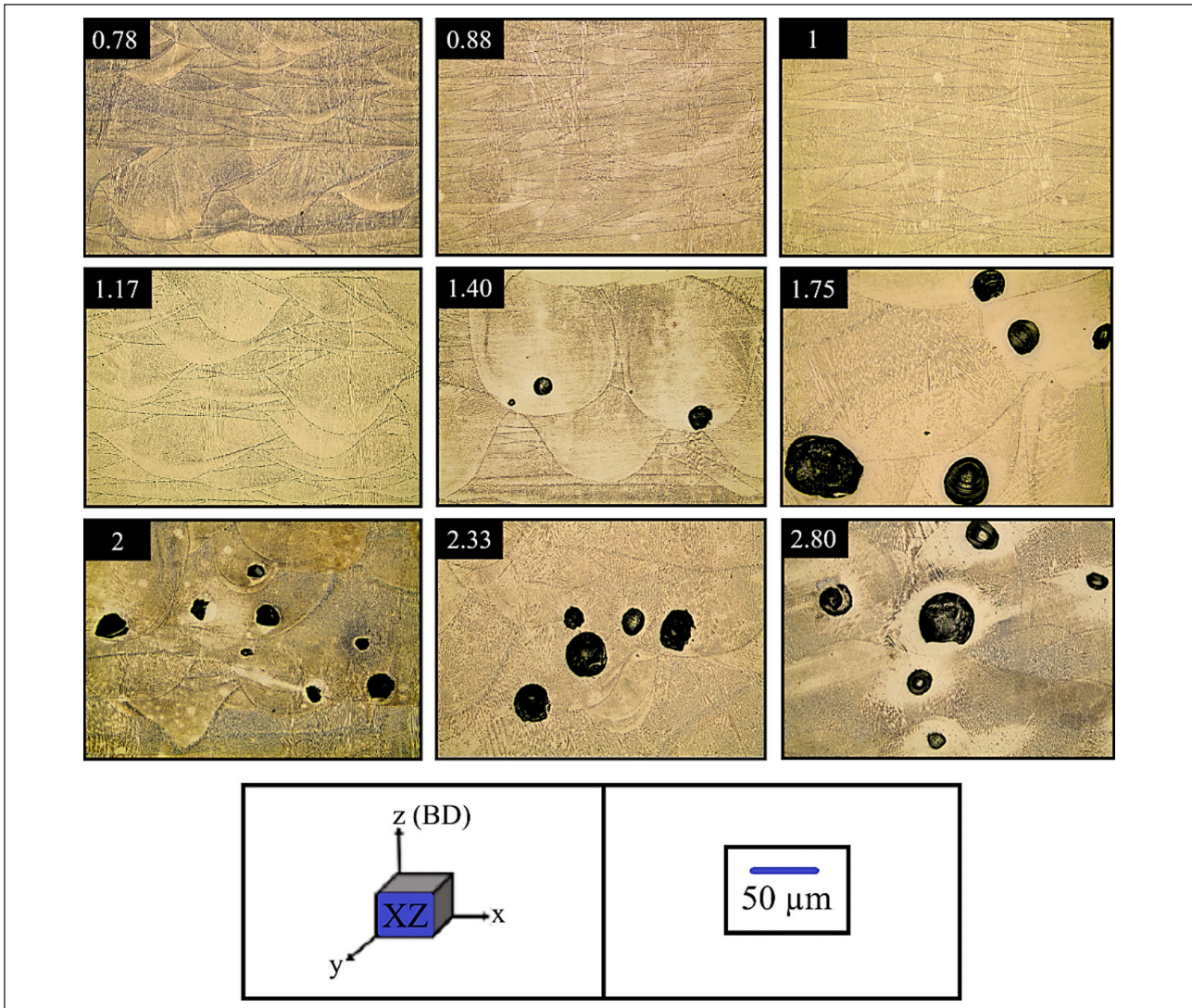**Figure 6**. Melt pool depth measurement.

Figure 7. Optical microscope image of the etched interface of the XZ plane according to LED values: The numbers in the upper left corner represent the LED values.

the samples produced with SLM is the 'Marangoni Convection' [42], leading to discontinuities in the microstructure. Marangoni convection is the reversal of the melt flow in the melt pool in the event of a local change in surface tension. This increase in surface tension from the centre of the heat source outwards can cause fluid flow circulation, called Marangoni convection. Marangoni convection tends to lower the temperature and change the melt pool geometry [46]. As a result of flow reversal, discontinuities and balling are observed in the microstructure. Increased scanning speed amplifies the impact of Marangoni convection and liquid capillary instability [47]. Therefore, the formation of Marangoni convection leads to a decrease in the mechanical properties of the material. Upon analysis of Figure 5, this particular type of crack was not observed. All samples in the study were created with a layer thickness of 30 μm. To regulate the thickness of the layer, the width of the melt pool was assessed at multiple points using the ImageJ software and then averaged. Figure 6 shows the regions where the melt

pool widths of IN625 alloy were measured and the average width value. The average of ten different melt pool depths was measured as 32 μm. Therefore, it is seen that the melt pool depths are compatible with the 30 μm layer thickness targeted in the study.

Figure 7 displays the presence of dendritic and coaxial growths in the microstructure, which can be attributed to variations in the cooling rate. The melt pool traces formed during laser beam scanning are readily observable in the microstructure. As a result of the scanning strategy, the melt pool traces seem to be partially overlapping. The microstructure exhibits cell-like and columnar dendritic formations. In addition, melt pool boundaries passing through the grain interiors were observed in the images. The etched images clearly demonstrate the porosities caused by high LED values (Fig. 7). In this respect, it is possible to say that the microstructure images and measured density results are compatible. According to the SLM machine and powder properties used in the study, the most suitable LED value for IN625 alloy was determined as 0.78 J/mm.

CONCLUSION

This study aims to clarify the impact of laser energy density on the porosity and microstructural characteristics of Inconel 625 alloy fabricated via selective laser melting (SLM) with a newly developed SLM metal additive manufacturing machine (ENAVISION 250, Ermaksan, Türkiye), for the first time. The main objective is to establish a clear correlation between the LED value and the porosity ratio, as well as to determine the optimal LED value for a layer thickness of 30 μm in the production of IN625 alloy. The critical findings of the study are summarised below.

- The highest relative density value was measured in the sample produced using an LED value of 0.78 J/mm (350 W laser power, 450 mm/s scanning speed) with 99.86%. Relative density values decreased with increasing LED value.
- Analysis of the microstructure images from the XY, XZ, and YZ planes revealed that the porosities within the structure increased after the LED value reached 1.17 J/mm. In addition, because of the increasing LED value, an increase in the pore size was also detected.
- The measurements of the melt pool width indicated that the intended layer thickness of 30 μm was achieved. This study successfully optimised the process, resulting in the production of the IN625 alloy via the SLM technique, achieving a density that closely aligns with the theoretical value.

The present study aims to reveal the effect of LED on porosity and microstructural features of the IN625 alloy produced by SLM using a newly developed SLM metal additive manufacturing machine (ENAVISION 250, Ermaksan, Türkiye), for the first time. The study mainly provides qualitative analysis regarding the impact of LED values on the porosity and microstructural characteristics of IN625 alloy, with statistical data included only to elucidate the final and relative density values of the samples in relation to LED values. Consequently, based on the data presented, it is recommended to conduct future experimental research to quantitatively assess the outcomes of this study, specifically examining the change of pore size and distribution in relation to LED values by statistical analysis. Future research should also focus on producing new materials with varying layer thicknesses, atmospheric condition, and powder characteristics utilising the ENAVISION 250 MAM machine, with the objective of fabricating critical components across multiple sectors, including aerospace, aviation, automotive, and defence industries.

Data Availability Statement

The authors confirm that the data that supports the findings of this study are available within the article. Raw data that support the finding of this study are available from the corresponding author, upon reasonable request.

Author's Contributions

Rıdvan Yamanoğlu: Conception, Design, Supervision, Interpretation, Critical Review.

Egemen Avcu: Conception, Design, Supervisior, Interpretation, Critical Review.

Hasan İsmail Yavuz: Conception, Design, Interpretation, Data Collection, Literature Review, Writer.

Mertcan Kıraç: Materials, Fundings, data collection and processing.

Ümit Gencay Başçı: Supervision, Design, Analysis and interpretation.

Enes Furkan Sevinç: Materials, Fundings, data collection and processing.

Ertuğrul Bayram: Materials, data collection and processing.

Conflict of Interest

The authors declared no potential conflicts of interest with respect to the research, authorship, and/or publication of this article.

Use of AI for Writing Assistance

Not declared.

Ethics

There are no ethical issues with the publication of this manuscript.

REFERENCES

[1] Başçı, Ü. G., & Yamanoğlu, R. (2021). New generation production technology: additive manufacturing via FDM. *International Journal of 3D Printing Technologies and Digital Industry, 5*(2), 339-352. [Turkish] [CrossRef]

[2] Altıparmak, S. C., & Xiao, B. (2021). A market assessment of additive manufacturing potential for the aerospace industry. *Journal of Manufacturing Processes, 68*, 728-738. [CrossRef]

[3] Mehrpouya, M., Dehghanghadikolaei, A., Fotovvati, B., Vosooghnia, A., Emamian, S. S., & Gisario, A. (2019). The potential of additive manufacturing in the smart factory industrial 4.0: A review. *Applied Sciences, 9*(18), Article 3865. [CrossRef]

[4] Frazier, W. E. (2014). Metal additive manufacturing: a review. *Journal of Materials Engineering and Performance, 23*, 1917-1928. [CrossRef]

[5] Kok, Y., Tan, X. P., Wang, P., Nai, M. L. S., Loh, N. H., Liu, E., & Tor, S. B. (2018). Anisotropy and heterogeneity of microstructure and mechanical properties in metal additive manufacturing: A critical review. *Materials & Design, 139*, 565-586. [CrossRef]

[6] Iakovakis, E., Avcu, E., Roy, M. J., Gee, M., & Matthews, A. (2022). Wear resistance of an additively manufactured high-carbon martensitic stainless steel. *Scientific Reports, 12*(1), Article 12554. [CrossRef]

[7] Moussaoui, K., Rubio, W., Mousseigne, M., Sultan, T., & Rezai, F. (2018). Effects of Selective Laser Melt-

ing additive manufacturing parameters of Inconel 718 on porosity, microstructure and mechanical properties. *Materials Science and Engineering: A, 735*, 182-190. [CrossRef]

[8] DebRoy, T., Wei, H. L., Zuback, J. S., Mukherjee, T., Elmer, J. W., Milewski, J. O., & Zhang, W. (2018). Additive manufacturing of metallic components-process, structure and properties. *Progress in Materials Science, 92*, 112-224. [CrossRef]

[9] Paraschiv, A., Matache, G., Condruz, M. R., Frigioescu, T. F., & Pambaguian, L. (2022). Laser powder bed fusion process parameters' optimization for fabrication of dense IN 625. *Materials, 15*(16), Article 5777. [CrossRef]

[10] Tonelli, L., Fortunato, A., & Ceschini, L. (2020). CoCr alloy processed by Selective Laser Melting (SLM): Effect of Laser Energy Density on microstructure, surface morphology, and hardness. *Journal of Manufacturing Processes, 52*, 106-119. [CrossRef]

[11] Başcı, Ü. G., & Yamanoğlu, R. (2022). Additive manufacturing via vat photopolymerization. *Düzce Üniversitesi Bilim ve Teknoloji Dergisi, 10*(2), 914-928. [Turkish] [CrossRef]

[12] Field, A. C., Carter, L. N., Adkins, N. J. E., Attallah, M. M., Gorley, M. J., & Strangwood, M. (2020). The effect of powder characteristics on build quality of high-purity tungsten produced via laser powder bed fusion (LPBF). *Metallurgical and Materials Transactions A, 51*, 1367-1378. [CrossRef]

[13] Harun, W. S. W., Kamariah, M. S. I. N., Muhamad, N., Ghani, S. A. C., Ahmad, F., & Mohamed, Z. (2018). A review of powder additive manufacturing processes for metallic biomaterials. *Powder Technology, 327*, 128-151. [CrossRef]

[14] Bascı, Ü.G. & Yamanoglu R. (2019). Eklemeli metal imalat teknolojileri için metal tozu üretim yöntemleri. *International Marmara Sciences* Congress (pp. 220-228). Kocaeli, Türkiye. [Turkish]

[15] Yap, C. Y., Chua, C. K., Dong, Z. L., Liu, Z. H., Zhang, D. Q., Loh, L. E., & Sing, S. L. (2015). Review of selective laser melting: Materials and applications. *Applied Physics Reviews, 2*(4), Article 041101. [CrossRef]

[16] Chowdhury, S., Yadaiah, N., Prakash, C., Ramakrishna, S., Dixit, S., Gupta, L. R., & Buddhi, D. (2022). Laser powder bed fusion: a state-of-the-art review of the technology, materials, properties & defects, and numerical modelling. *Journal of Materials Research and Technology, 20*, 2109-2172. [CrossRef]

[17] Gu, D., & Shen, Y. (2009). Effects of processing parameters on consolidation and microstructure of W-Cu components by DMLS. *Journal of Alloys and Compounds, 473*(1-2), 107-115. [CrossRef]

[18] Yadroitsev, I., Krakhmalev, P., Yadroitsava, I., Johansson, S., & Smurov, I. (2013). Energy input effect on morphology and microstructure of selective laser melting single track from metallic powder. *Journal of Materials Processing Technology, 213*(4), 606-613. [CrossRef]

[19] Larimian, T., Kannan, M., Grzesiak, D., AlMangour, B., & Borkar, T. (2020). Effect of energy density and scanning strategy on densification, microstructure and mechanical properties of 316L stainless steel processed via selective laser melting. *Materials Science and Engineering: A, 770*, Article 138455. [CrossRef]

[20] Ma, M., Wang, Z., & Zeng, X. (2015). Effect of energy input on microstructural evolution of direct laser fabricated IN718 alloy. *Materials Characterization, 106*, 420-427. [CrossRef]

[21] Greco, S., Gutzeit, K., Hotz, H., Kirsch, B., & Aurich, J. C. (2020). Selective laser melting (SLM) of AISI 316L-impact of laser power, layer thickness, and hatch spacing on roughness, density, and microhardness at constant input energy density. *The International Journal of Advanced Manufacturing Technology, 108*, 1551-1562. [CrossRef]

[22] Wang, W., Wang, S., Zhang, X., Chen, F., Xu, Y., & Tian, Y. (2021). Process parameter optimization for selective laser melting of Inconel 718 superalloy and the effects of subsequent heat treatment on the microstructural evolution and mechanical properties. *Journal of Manufacturing Processes, 64*, 530-543. [CrossRef]

[23] Sadowski, M., Ladani, L., Brindley, W., & Romano, J. (2016). Optimizing quality of additively manufactured Inconel 718 using powder bed laser melting process. *Additive Manufacturing, 11*, 60-70. [CrossRef]

[24] Yi, J. H., Kang, J. W., Wang, T. J., Wang, X., Hu, Y. Y., Feng, T., ... & Wu, P. Y. (2019). Effect of laser energy density on the microstructure, mechanical properties, and deformation of Inconel 718 samples fabricated by selective laser melting. *Journal of Alloys and Compounds, 786*, 481–488. [CrossRef]

[25] Bertoli, U. S., Wolfer, A. J., Matthews, M. J., Delplanque, J. P. R., & Schoenung, J. M. (2017). On the limitations of volumetric energy density as a design parameter for selective laser melting. *Materials & Design, 113*, 331-340. [CrossRef]

[26] Bascı, U.G. & Yamanoğlu R. (2020). Eklemeli metal imalat teknolojileri ve uygulama alanları. *International Marmara Sciences* Congress (pp. 307-314). Kocaeli, Türkiye. [Turkish]

[27] Spierings, A. B., Schneider, M. U., & Eggenberger, R. (2011). Comparison of density measurement techniques for additive manufactured metallic parts. *Rapid Prototyping Journal, 17*(5), 380-386. [CrossRef]

[28] Fayazfar, H., Salarian, M., Rogalsky, A., Sarker, D., Russo, P., Paserin, V., & Toyserkani, E. (2018). A critical review of powder-based additive manufacturing of ferrous alloys: Process parameters, microstructure and mechanical properties. *Materials & Design, 144*, 98-128. [CrossRef]

[29] Gor, M., Soni, H., Wankhede, V., Sahlot, P., Grzelak K., Szachgluchowicz I., & Kluczyński J. (2021). A critical review on effect of process parameters on mechanical and microstructural properties of powder-bed fusion additive manufacturing of SS316L. *Materials, 14*(21), Article 6527. [CrossRef]

[30] Kladovasilakis, N., Charalampous, P., Kostavelis, I., Tzetzis, D., & Tzovaras, D. (2021). Impact of metal additive manufacturing parameters on the powder bed fusion and direct energy deposition processes: A comprehensive review. *Progress in Additive Manufacturing, 6*, 349-365. [CrossRef]

[31] Pleass, C., & Jothi, S. (2018). Influence of powder characteristics and additive manufacturing process parameters on the microstructure and mechanical behaviour of Inconel 625 fabricated by Selective Laser Melting. *Additive Manufacturing, 24*, 419-431. [CrossRef]

[32] Oliveira, J. P., LaLonde, A. D., & Ma, J. (2020). Processing parameters in laser powder bed fusion metal additive manufacturing. *Materials & Design, 193*, Article 108762. [CrossRef]

[33] Sefene, E. M. (2022). State-of-the-art of selective laser melting process: A comprehensive review. *Journal of Manufacturing Systems, 63*, 250-274. [CrossRef]

[34] Dietrich, K., Diller, J., Dubiez-Le Goff, S., Bauer, D., Forêt, P., & Witt, G. (2020). The influence of oxygen on the chemical composition and mechanical properties of Ti-6Al-4V during laser powder bed fusion (L-PBF). *Additive Manufacturing, 32*, Article 100980. [CrossRef]

[35] Sutton, A. T., Kriewall, C. S., Leu, M. C., & Newkirk, J. W. (2017). Powder characterisation techniques and effects of powder characteristics on part properties in powder-bed fusion processes. *Virtual and Physical Prototyping, 12*(1), 3-29. [CrossRef]

[36] Kokareva, V. V., Smelov, V. G., Agapovichev, A. V., Sotov, A. V., & Sufiiarov, V. S. (2018). Development of SLM quality system for gas turbines engines parts production. In *IOP Conference Series: Materials Science and Engineering, 441*(1), Article 012024. [CrossRef]

[37] Ravichander, B. B., Mamidi, K., Rajendran, V., Farhang, B., Ganesh-Ram, A., Hanumantha, M., Amerinatanzi, A. (2022). Experimental investigation of laser scan strategy on the microstructure and properties of Inconel 718 parts fabricated by laser powder bed fusion. *Materials Characterization, 186*, Article 111765. [CrossRef]

[38] Yamanoglu, R., Bahador, A., & Kondoh, K. (2023). Support recycling in additive manufacturing: A case study for enhanced wear performance of Ti6Al4V alloy. *Proceedings of the Institution of Mechanical Engineers, Part J: Journal of Engineering Tribology,* *237*(7), 1603-1608. [CrossRef]

[39] Du, C., Zhao, Y., Jiang, J., Wang, Q., Wang, H., Li, N., & Sun, J. (2023). Pore defects in Laser Powder Bed Fusion: Formation mechanism, control method, and perspectives. *Journal of Alloys and Compounds, 944*, Article 169215. [CrossRef]

[40] Wang, L., Zhang, Y., Chia, H. Y., & Yan, W. (2022). Mechanism of keyhole pore formation in metal additive manufacturing. *NPJ Computational Materials, 8*(1), Article 22. [CrossRef]

[41] Sanaei, N., & Fatemi, A. (2021). Defects in additive manufactured metals and their effect on fatigue performance: A state-of-the-art review. *Progress in Materials Science, 117*, Article 100724. [CrossRef]

[42] Narasimharaju, S. R., Zeng, W., See, T. L., Zhu, Z., Scott, P., Jiang, X., & Lou, S. (2022). A comprehensive review on laser powder bed fusion of steels: Processing, microstructure, defects and control methods, mechanical properties, current challenges and future trends. *Journal of Manufacturing Processes, 75*, 375-414. [CrossRef]

[43] Sing, S. L., An, J., Yeong, W. Y., & Wiria, F. E. (2016). Laser and electron-beam powder-bed additive manufacturing of metallic implants: A review on processes, materials and designs. *Journal of Orthopaedic Research, 34*(3), 369-385. [CrossRef]

[44] Song, B., Zhao, X., Li, S., Han, C., Wei, Q., Wen, S., ... & Shi, Y. (2015). Differences in microstructure and properties between selective laser melting and traditional manufacturing for fabrication of metal parts: A review. *Frontiers of Mechanical Engineering, 10*, 111-125. [CrossRef]

[45] Ding, H., Zhang, J., Liu, J., Wang, J., Niu, L., & Chen, Y. (2023). Effect of volume energy density on microstructure and mechanical properties of TC4 alloy by selective laser melting. *Journal of Alloys and Compounds, 968*, Article 171769. [CrossRef]

[46] Yusuf, S. M., & Gao, N. (2017). Influence of energy density on metallurgy and properties in metal additive manufacturing. *Materials Science and Technology, 33*(11), 1269-1289. [CrossRef]

[47] Fousová, M., Vojtěch, D., Kubásek, J., Jablonská, E., & Fojt, J. (2017). Promising characteristics of gradient porosity Ti-6Al-4V alloy prepared by SLM process. *Journal of the Mechanical Behavior of Biomedical Materials, 69*, 368-376. [CrossRef]